Hindawi
Mathematical Problems in Engineering
Volume 2019, Article ID 2152858, 9 pages
https://doi.org/10.1155/2019/2152858

Research Article

A Method of Enhancing Fast Steering Mirror's Ability of Anti-Disturbance Based on Adaptive Robust Control

Shitao Zhang[1,2] **Bao Zhang**[1] **Xiantao Li**[1] **Zhengxi Wang**[1,2] **and Feng Qian**[1]

[1] *Changchun Institute of Optics, Fine Mechanics and Physics, Chinese Academy of Sciences, #3888 Dongnanhu Road, Changchun 130033, China*
[2] *University of Chinese Academy of Science, #19 Yuquan Road, Beijing 100049, China*

Correspondence should be addressed to Bao Zhang; zhangb@ciomp.ac.cn

Received 27 April 2018; Revised 6 December 2018; Accepted 23 December 2018; Published 6 January 2019

Academic Editor: Francesco Aggogeri

Fast steering mirror (FSM) plays a crucial role in stabilization of the line-of-sight (LOS) and phase shift compensation. The control accuracy of the FSM is affected by various disturbances especially the vibration in the aviation environment. Traditional anti-disturbance methods, such as disturbance observer (DOB), have a little effect of suppressing disturbance in FSM. But it also brings some problem, such as increasing mass and amplifying high frequency noise. To solve these problems, an anti-disturbance strategy based on adaptive robust control (ARC) was proposed. And it will not amplify the high-frequency noise which is inevitable in DOB. Experimental results show that, using adaptive robust controller, the steady-state error of the FSM decreased 4.8 times compared to simple PID control and 1.9 times compared to DOB+PID control in the simulated vibration environment.

1. Introduction

As a mirror device for controlling the direction of light beam between a target and a receiver, FSM has been widely used in optical systems such as telescopes, laser communications, image stabilization, and precise tracking and aiming [1–3]. In the aerial photoelectric stabilized platform, FSM is mainly used to stabilize the LOS and compensate the imaging phase shift [4]. However, FSM's control accuracy will be seriously affected by aircraft position fluctuations caused by the air current, engine vibration, and other disturbances. Therefore, effective disturbance rejection methods need to be proposed to enhance the robustness of FSM [2].

As shown in Table 1, there are three main types of anti-disturbance strategies of FSM. The first method is to use piezoelectric ceramics as actuator to drive FSM [5]. Piezoelectric ceramics have strong robustness and high control bandwidth due to their special structure. However, the motion range of such FSM is relatively small as a result of the motion mechanism of the piezoelectric ceramic. This seriously limits the performance of FSM in terms of stabilization of LOS and phase compensation. The second method is to add reaction mass [6]. Eccentric torque caused by external disturbance can be reduced by this method. But it will increase the mass of FSM and then amplify the difficulty of driver. The third method is anti-disturbance algorithm [7, 8]. Compared with previous methods, this method is simpler and more effective for it won't change the structure or add extra mass.

DOB [9–11] and various improved algorithms based on it are widely used in FSM. For example, the EDOB [7] proposed by Chao Deng. In addition, Jing Tian [8] proposed a method based on acceleration loop to improve the anti-disturbance ability of FSM. But these methods both require an acceleration loop which needs accelerometer. The introduction of accelerometers will increase the mass and cost of FSM. Furthermore, DOB will amplify high frequency noise, which strongly influences the performance of the control system.

To solve these problems, ARC is adopted in this paper to suppress disturbance of FSM. ARC, an anti-disturbance control algorithm combining SMC and AC, was proposed by Bin Yao [12–14] in 1996. It possesses both the adaptability of AC [15, 16] for model uncertainty and the ability of SMC

Table 1: Existing anti-disturbance method of FSM.

METHODS	AUTHOR	ADVANTAGE	DISADVANTAGE
PIEZOELECTRIC ACTUATOR	Harry Marth [5]	Strong Robustness;	Overweight; Small Angular Range
REACTION MASS	Andrew Bullard [6]	Insensitive to Eccentric Torque	Overweight; Difficult to Design,
ANTI-DISTURBANCE ALGORITHM	Chao Deng [7]	Without Adding Weight; Suit to Different Structure	Need Another Sensor; Low Effective Bandwidth

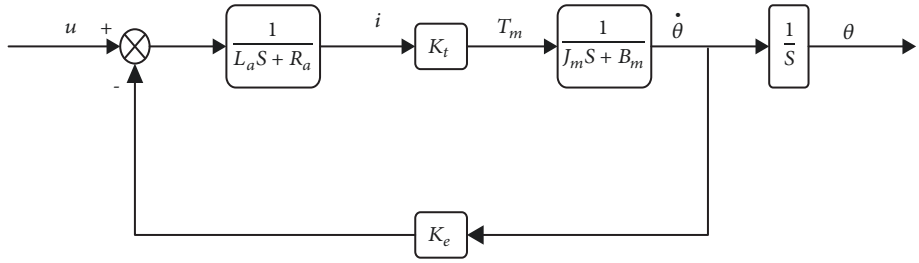

Figure 1: Model structure diagram.

[17–20] for suppressing disturbance. In addition, acceleration loop is not necessary for ARC and it will not amplify the high frequency noise, compared with DOB.

The aim of this study is to design adaptive robust controller for FSM and analyze the comparative experimental results of ARC and DOB. In previous design, an accurate modeling method was proposed and used to model the FSM. This paper is organized as follows: Section 2 presents a detailed introduction of FSM modeling, mainly describing the method of model correcting. Section 3 discusses and analyzes the impact of disturbance and DOB. Section 4 introduces the design process of ARC. Section 5 sets up the experiments used to verify this method and analyzes the experimental result. Concluding remarks are presented in Section 6.

2. System Identification and Model Correcting

2.1. System Identification. In Figure 1 , u is the input voltage signal, θ is the output angle, L_a is the armature inductance, R_a is the armature resistance, i is the armature current, K_t is the electromagnetic torque constant, T_m is the motor output torque, J_m is the motor moment of inertia, B_m is the motor side viscous damping coefficient, $\dot{\theta}$ is the angular velocity, and K_e is the back-EMF coefficient.

As the actuator of FSM, voice coil motor is the main target for modeling the FSM. Theoretical model of FSM is shown in Figure 1. And white noise sweep is used to model the FSM. The amplitude-frequency response and the phase-frequency response curve of FSM's open-loop model are shown in the blue line in Figure 2. A simple second-order model, shown in Figure 2 (green line), can be fitted according to the White Noise Sweep data by Matlab System Identification Toolbox. However, this modeling method is relatively crude, and the model curve cannot be matched with the actual model curve

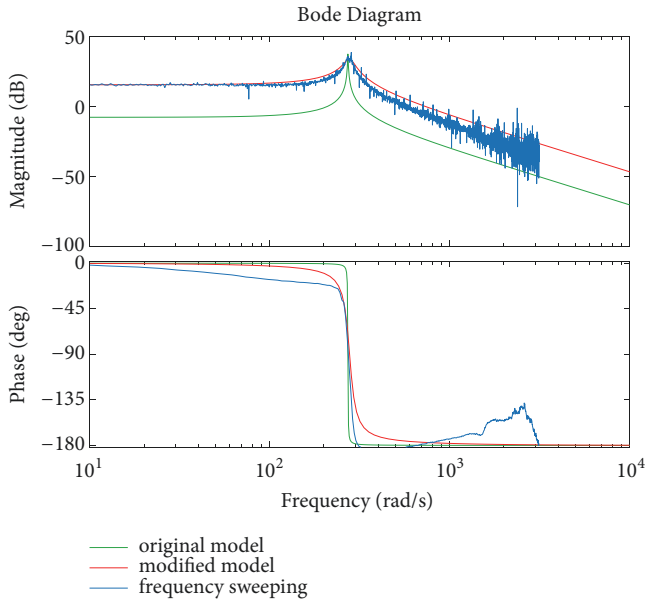

Figure 2: Comparative curve of swept frequency and fit.

(frequency sweeping curve). Therefore, the original model needs to be modified.

There are many ways to do this. In this study, step response matching method was applied to manually modify the original model. By comparing the simulative step curve with the actual step curve, the difference between the mathematical model and the actual model was detected, and then the model was gradually adjusted so that the model's simulative curve gradually approaches the actual step curve. It can be seen from Figure 2 that the curve (red line) after manual modified basically matches the frequency sweeping curve (blue line), which proves that the modeling method is of high accuracy. Equation (1) is the modified model.

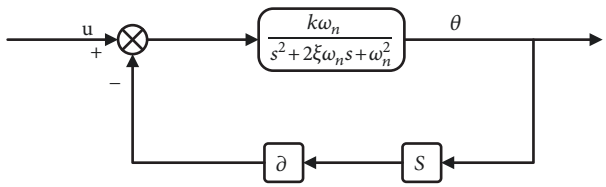

Figure 3: Schematic diagram of differential feedback compensation.

$$\frac{455000}{S^2 + 32.5S + 77000} \tag{1}$$

2.2. Model Correcting. It can be seen from Figure 2 that there is a second-order resonant peak in the amplitude-frequency curve of FSM model. And it will result in system chattering when FSM is in closed-loop control. In order to obtain high control performance, it is necessary to suppress the second-order resonance of the model.

According to the character of second-order system, the differential feedback compensation shown in Figure 3 was proposed. The FSM model became equation (2), after compensation component was introduced.

$$\frac{k\omega_n}{S^2 + (2\xi\omega_n + \alpha k\omega_n) S + \omega_n^2} \tag{2}$$

Equation (2) shows that damping coefficient of this system can be adjusted by changing the value of α. And the system resonance will be suppressed by increasing the damping coefficient. As shown in Figure 4, system resonant peak is eliminated after the differential feedback compensation component was introduced.

3. Traditional Anti-Disturbance Methods

3.1. Disturbance Analysis. FSM is affected by various external disturbances, including aircraft engine vibration, aircraft posture fluctuations caused by air turbulence, and model changes caused by overweight and weightlessness. The vibration, which has the most significant interference with the FSM, is the main research focus of anti-disturbance algorithm. d is used to represent the total external disturbance in this paper. System control block diagram containing the disturbance d is shown in Figure 5.

$G_c(s)$ is the controller and $G_p(s)$ is the plant model. Suppose the ideal output without external disturbances is θ_i and the output of external disturbances d is θ_d.

$$\begin{aligned} \theta_i &= G_{u\theta}(s)\, u \\ \theta_d &= G_{d\theta}(s)\, d \end{aligned} \tag{3}$$

where

$$\begin{aligned} G_{u\theta}(s) &= \frac{G_c(s) G_p(s)}{1 + G_c(s) G_p(s)} \\ G_{d\theta}(s) &= \frac{G_p(s)}{1 + G_c(s) G_p(s)} \end{aligned} \tag{4}$$

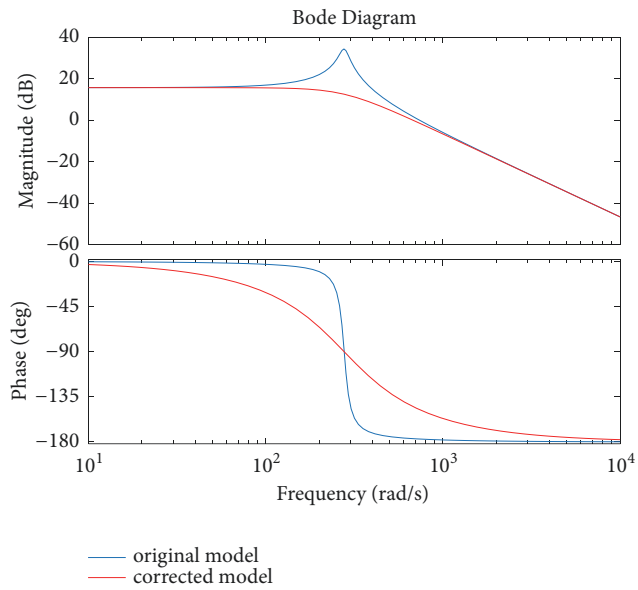

Figure 4: Comparison of model before and after correction.

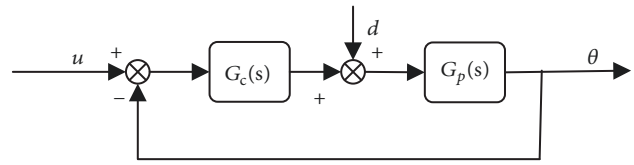

Figure 5: Control structure with disturbance.

The actual output of the system is θ.

$$\begin{aligned} \theta = \theta_i + \theta_d &= \frac{G_c(s) G_p(s)}{1 + G_c(s) G_p(s)} u + \frac{G_p(s)}{1 + G_c(s) G_p(s)} d \\ &= \frac{G_p(s)\left(G_c(s)\, u - d\right)}{1 + G_c(s) G_p(s)} \end{aligned} \tag{5}$$

From (5), it can be seen that the disturbance would affect the output through the model and cause the actual output to deviate from the ideal output. Although increasing the amplitude of the controller can minimize the influence of the disturbance, due to the limitation of the control system and the mechanical resonance, the amplitude of the controller cannot be increased indefinitely. So it is necessary to introduce another anti-disturbance control method into the system besides PID controller.

3.2. Disturbance Observer. Disturbance observer designed according to the principle of intima is the most common anti-disturbance control algorithm. The basic principle of DOB is using the nominal model to estimate the difference between the actual output and the ideal output. Based on this, disturbance can be observed and compensated into the controller. The basic schematic is as in Figure 6.

$G_{pn}(s)$ is the nominal model, $Q(s)$ is the low-pass filter, $\hat{d}$ is the DOB estimated disturbance, and ξ is the detection

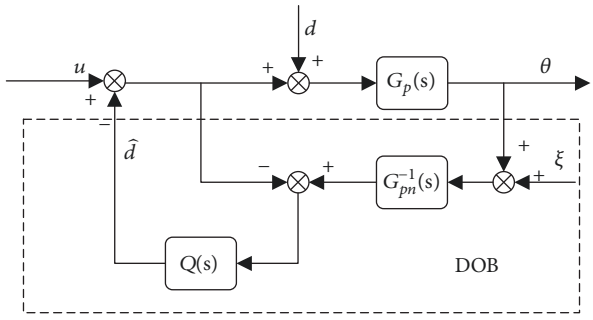

Figure 6: Disturbance observer.

noise. The relationship between input and output is given as equation (6), as shown in Figure 6.

$$\theta(s) = G_{u\theta}(s)\,u(s) + G_{d\theta}(s)\,d(s) + G_{\xi\theta}(s)\,\xi(s) \tag{6}$$

where

$$\begin{aligned} G_{u\theta}(s) &= \frac{G_{pn}(s)\,G_p(s)}{G_{pn}(s) + \left(G_p(s) - G_{pn}(s)\right)Q(s)} \\ G_{d\theta}(s) &= \frac{G_{pn}(s)\,G_p(s)\,(1 - Q(s))}{G_{pn}(s) + \left(G_p(s) - G_{pn}(s)\right)Q(s)} \\ G_{\xi\theta}(s) &= \frac{G_p(s)\,Q(s)}{G_{pn}(s) + \left(G_p(s) - G_{pn}(s)\right)Q(s)} \end{aligned} \tag{7}$$

In the ideal case, the low-pass filter Q(s) has a gain of 1 at low frequency. Then

$$\begin{aligned} &G_{u\theta}(s) \approx G_{pn}(s), \\ &G_{d\theta}(s) \approx 0, \\ &G_{\xi\theta}(s) \approx 1 \end{aligned} \tag{8}$$

Under such circumstance, disturbance d has no effect on output θ and the system's external equivalent disturbance is completely suppressed, but the detection noise is passed through the filter to the output without restriction. At the same time, in order to suppress the high-frequency noise of the position sensor, it is necessary that $Q(s)$ has a gain of 0 at high frequency. However, in practical engineering applications, this ideal situation does not exist for the following three problems:

(1) In order to suppress the high-frequency disturbance, the cut-off frequency of the low-pass filter is required to be as high as possible; but at the same time, the cut-off frequency should be as low as possible to suppress the high-frequency detection noise of the sensor. This is the biggest contradiction of DOB in application process.

(2) There is no ideal low-pass filter. The transition zone between passband and stopband is inevitable in practical filters. And the effect of filtering is terrible in transition zone, because in this zone the low frequency gain is not 1; and the high-frequency gain is not 0.

(3) Although a precise modeling method was used in this study, it does not guarantee that nominal model $G_{pn}(s)$ is exactly equal to the actual model $G_p(s)$. This model error would result in undercompensation or overcompensation of disturbance.

In summary, although DOB has many advantages including simple principle and suitable for most situations, several problems come with it in practical engineering application restrict its performance of anti-disturbance.

4. Design of Adaptive Robust Controller

Using conventional DOB control strategies to suppress the effects of external disturbances (mainly vibration) in FSM control system was introduced in Section 3. As mentioned there, due to problems exist in DOB, the external disturbances were not restrained well (the experimental results of DOB are shown in Section 5). ARC, a more effective anti-disturbance control algorithm, is introduced in this section. The control block diagram is shown in Figure 7.

The relationship between input u and output θ can be obtained as:

$$\begin{aligned} J\ddot{\theta} + B\dot{\theta} + C\theta &= u + d \\ or\ \theta &= G_p(s)\,(u + d) \\ G_p(s) &= \frac{1}{Js^2 + Bs + C} \end{aligned} \tag{9}$$

where J is the inertia, B is the velocity damping coefficient, and C is the elastic damping coefficient. The objective is to synthesize a control input such that the resulting system from μ to θ behaves like its nominal model; i.e., we want

$$\begin{aligned} J_n\ddot{\theta} + B_n\dot{\theta} + C_n\theta &= \mu \\ or\ \theta &= G_{pn}(s)\,\mu \\ G_{pn}(s) &= \frac{1}{J_n s^2 + B_n s + C_n} \end{aligned} \tag{10}$$

where J_n B_n, and C_n are the nominal values of J B, and C. For simplicity, in this section, we assume that the variations of J B, and C are not so big that their effects can be neglected; i.e., $J = J_n$ $B = B_n$, and $C = C_n$ in the following.

Define a switching-function-like quantity p as

$$p = \dot{\theta} + \lambda\theta - \frac{1}{J_n}\int_0^t \mu(\tau)\,d\tau + \frac{C_n}{J_n}\int_0^t \theta(\tau)\,d\tau \tag{11}$$

where $\lambda = B_n/J_n$ from (12) and (14),

$$J_n\dot{p} = u + d - \mu \tag{12}$$

If $\dot{p} = 0$ (or sliding mode called in the field of sliding mode control), ideal relationship of input-output can be obtained

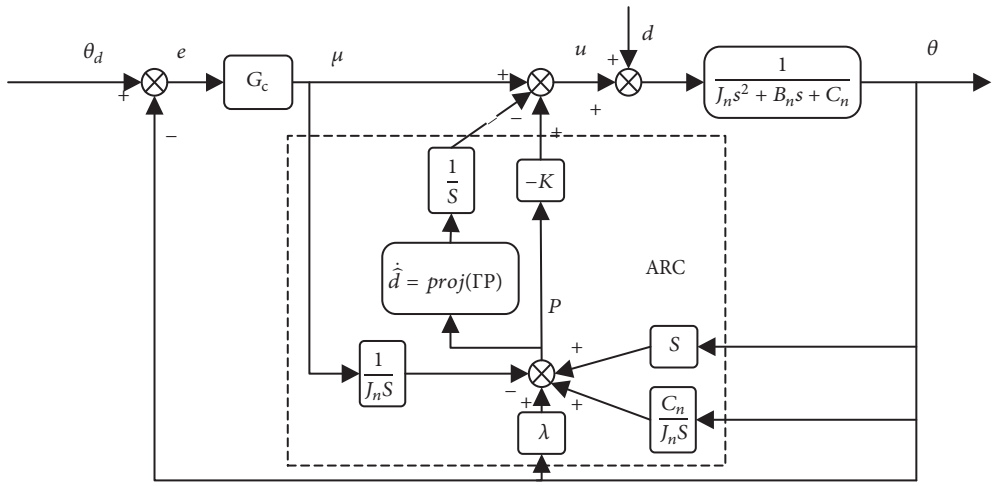

Figure 7: Adaptive robust controller.

and the effect of external disturbances on the system is negligible. However, due to the problem of system causality (the relationship between $\dot{p}$ and u is static), $\dot{p} = 0$ is not practical. The best we can do is to make $\dot{p}$ as small as possible in the feedback system. If all signals contained by p are uniformly continuous, then $p \longrightarrow 0$ means $\dot{p} \longrightarrow 0$. In a sense small p means small $\dot{p}$ [12, 16]. So in the following, we are going to synthesize u such that p is as small as possible.

Design control law as

$$\begin{aligned} u &= u_s + u_d, \\ u_s &= -Kp, \\ u_d &= \mu - \hat{d} \end{aligned} \tag{13}$$

where $K > 0$ and $\hat{d}$ is the estimate of total external disturbance. Let d_M and d_m be the upper and lower boundaries of the disturbance, respectively.

$$d \in (\mathrm{d}_m, \mathrm{d}_M) \tag{14}$$

Substituting (13) into (12), the error is

$$J_n \dot{p} + Kp = -\dot{d} \tag{15}$$

where $\dot{d} = \hat{d} - d$ is the estimation error. If $\dot{d}$ is treated as input and p is treated as output, (15) can be considered as a first-order system. It can be known by the first-order systematic characteristic that $|p(\infty)| \le \dot{d}\ (\infty)/\mathrm{K}$. Therefore as long as the value of K increases, the value of p decreases. It is also the most common strategy in robust control to improve the robustness of the control system by using a simplified specific control structure and increasing the feedback coefficient. However, in practical control system, the value of K cannot be increased indefinitely because of system's chattering and mechanical resonance. When K increases to the upper limit, the value of the p will depend on the value of $\dot{d}$. Therefore, in order to further improve the performance of the system, adaptive control method was introduced to decrease the value of the estimated error $\dot{d}$.

The expression of adaptive law is

$$\dot{\hat{d}} = \begin{cases} 0, & if \begin{cases} \hat{d} = d_M & and\ p > 0 \\ \hat{d} = d_m & and\ p < 0 \end{cases} \\ \Gamma p, & otherwise \end{cases} \tag{16}$$

where $\Gamma > 0$ is the adaptive coefficient. It can be shown that the above type of adaptation law guarantees that

$$\hat{d} \in (\mathrm{d}_m, \mathrm{d}_M) \tag{17}$$

All in all, if the external disturbance d is a fixed value, then the value of $\hat{d}$ could infinitely approach the value of d and finally eliminate the estimation error $\dot{d}$ under the control of ARC through adaptive algorithm regardless of the value of K. If the external disturbance d is variable, then the adaptive coefficient Γ needs to be increased to match the variety rate of d. But the value of Γ related to K cannot increase without limitation. Therefore, this adaptive law can deal with low-frequency disturbances well. For high-frequency disturbances, its performance is limited by the upper limit of Γ.

5. Comparative Experiments and Discussion

5.1. Comparative Experiments. The vibration platform was used to simulate the external disturbances (because the main disturbance is the vibration), then the PID, PID + DOB, and PID + ARC control algorithms were tested, respectively.

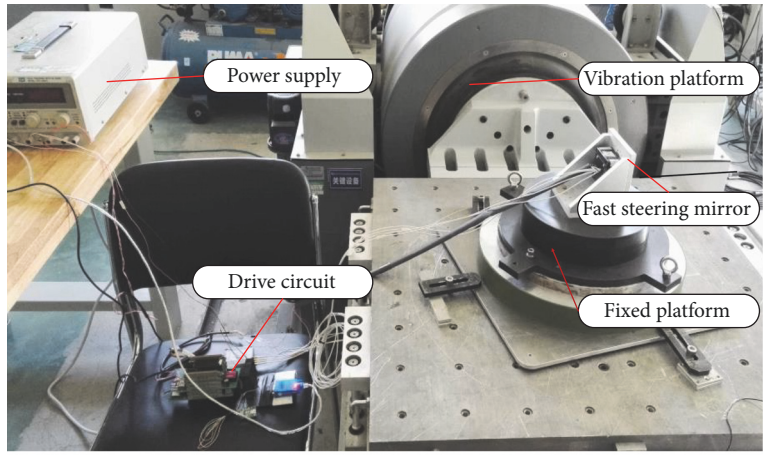

Figure 8: Experimental apparatus.

Experimental equipments are shown in Figure 8. Random vibration containing many kinds of frequencies was adopted to simulate actual vibration, among which the amplitude of low frequency is relatively large and the amplitude of high frequency is relatively small. Its average value is 5G, and only 1.8G was delivered to FSM over the Fix Platform.

First of all, the stability of these three control methods was tested without vibration, as shown in Figure 9. Then, the anti-disturbance ability of these three control methods was tested under the vibration condition. The time-domain curves are shown in Figure 10 and the frequency response curves are shown in Figure 11.

5.2. Discussion. The error curves of FSM under the control of these three kinds of control methods are shown in Figure 9. The maximum, average, and root-mean-square values of these three error curves are tabulated in Table 2. It can be seen from Figure 9 and Table 2 that the stability of PI and PI + ARC control method was better at static state, and the RMS of error were 1.6938 and 2.8877, respectively. However, the stability of PID + DOB control method was relatively poor, and the RMS of error was 33.4699. The high frequency noise mentioned in Section 2 was the main reason for this result. The amplified high frequency noise eventually resulted in a larger position error of FSM.

The time-domain error curves of these three control methods under the vibration condition are shown in Figure 10. Their maximum, average, and root-mean-square values are shown in Table 3, and these frequency-domain error curves are shown in Figure 11. A discussion about the ability of the three control methods is given next.

(1) PID: The maximum error of the system output was 290.0618 and the RMS was 82.4228 under the control of the traditional PID controller. The spectral components of error were mainly focused within 100Hz, and it had the maximum error at 20Hz.

(2) DOB: The anti-disturbance ability of the system had been improved, and the maximum error decreased 1.78 times to 163.1598; the RMS decreased 1.9 times to 43.2125 after adding DOB controller into the control system. Although the low-frequency components were suppressed, some residuals still exist. The high-frequency components became obvious due to the noise amplification. The peak frequency of magnitude was about 200 Hz at which magnitude was magnified 5.2 times.

(3) ARC: The anti-disturbance ability of the FSM had been significantly improved, and the maximum error decreased 4.86 times to 59.6489; RMS decreased 4.83 times to 17.0788, after adding the ARC controller into control system. The low-frequency components were significantly suppressed, the peak value decreased 8.1 times, and the high-frequency components had not been amplified.

In summary, it had little influence on the control accuracy to add ARC controller into control system when it is in static state. But the control precision of the system was affected by the amplification of high-frequency noise after adding the DOB controller. Although both control methods can improve the anti-disturbance ability of the control system when FSM is in a vibration environment, the experimental results show that ARC's performance of anti-disturbance was better than DOB's and it would not amplify the high-frequency noise.

6. Conclusions

The control accuracy of FSM was highly sensitive to disturbance especially vibrations in aviation environment. DOB, the traditional anti-disturbance method, was analyzed, and the results show that it would amplify the high-frequency noise. In this paper, ARC preserving the advantage of deterministic robust control and adaptive control while removing their drawbacks was proposed to improve the anti-disturbance ability of FSM. And two sets of control experiments were made to compare the performances of these three control methods. Experimental results show that the control accuracy of DOB was the worst in static state;

Table 2: Control precision contrast under static conditions.

Control methods	MAX [1]	MEAN [2]	RMS [3]
PID(urad)	8.1872	1.0041	1.6938‘
PID+DOB(urad)	67.8370	27.2953	33.4699
PID+ARC(urad)	9.3568	1.9641	2.8877

1 MAX stands for largest elements in the error.
2 MEAN stands for average deviation of the error.
3 RMS stands for root mean square of the error.

Table 3: Control precision contrast under vibration conditions.

Control methods	MAX [1]	MEAN [2]	RMS [3]
PID(urad)	290.0618	67.3275	82.4228
PID+DOB(urad)	163.1598	34.4581	43.2125
PID+ARC(urad)	59.6498	13.4877	17.0788

1 MAX stands for largest elements in the error.
2 MEAN stands for average deviation of the error.
3 RMS stands for root mean square of the error.

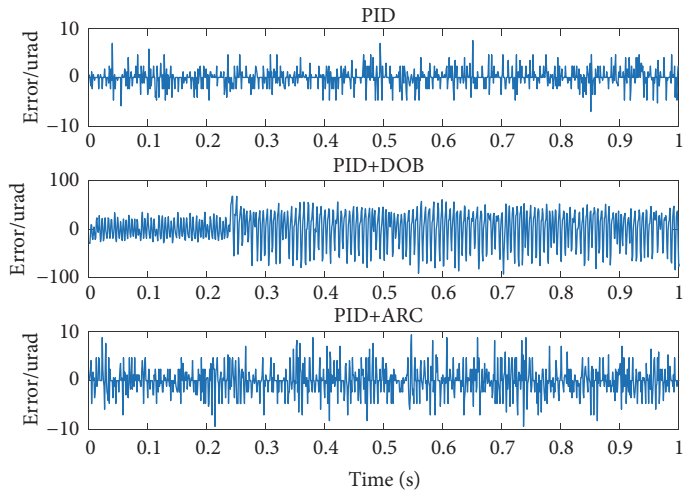

Figure 9: Time domain contrast curve under static conditions.

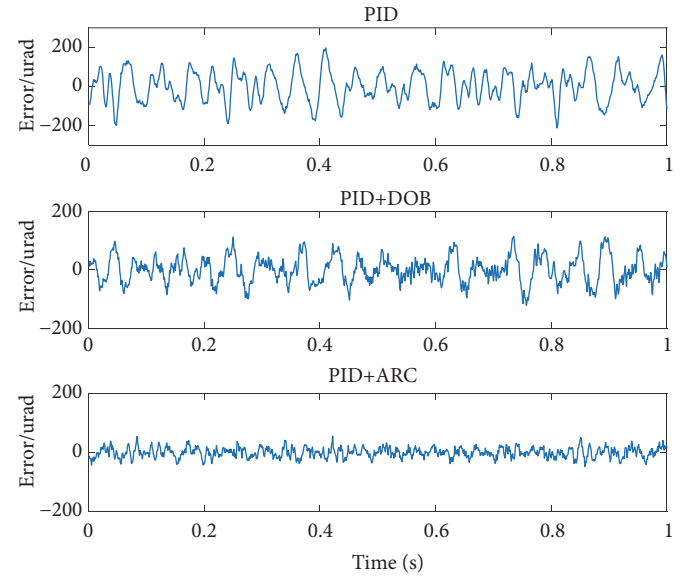

Figure 10: Time domain contrast curve under vibration condition.

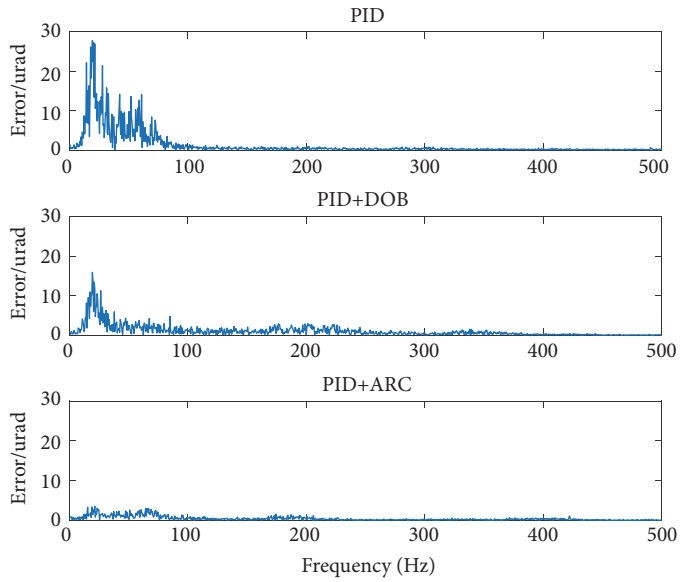

Figure 11: Frequency domain contrast curve under vibration condition.

Table 4: List of acronyms.

FSM	Fast Steering Mirror
LOS	Line-of-Sight
DOB	Disturbance Observer
PID	Proportion Integral Differential
ARC	Adaptive Robust Control
AC	Adaptive Control
SMC	Sliding Model Control

and ARC had the best effect on suppressing disturbance in simulated vibration environment.

Appendix

See Table 4.

Data Availability

The data that support the findings of this study are available on request from the corresponding author. The data are not publicly available due to restrictions, e.g., them containing information that could compromise the privacy of research participants.

Conflicts of Interest

The authors declare that they have no conflicts of interest.

References

[1] X. Li, B. Zhang, H. Shen, and D. Tian, "The booting-Type ADRC of airborne photoelectrical platform," *Mathematical Problems in Engineering*, vol. 2014, p. 9, 2014.

[2] N. Chen, B. Potsaid, J. T. Wen, S. Barry, and A. Cable, "Modeling and control of a fast steering mirror in imaging applications," in *Proceedings of the 2010 IEEE International Conference on Automation Science and Engineering (CASE 2010)*, pp. 27–32, Toronto, ON, Canada, August 2010.

[3] L. R. Hedding, "Fast steering mirror design and performance for stabilization and single axis scanning," in *Proceedings of the 1990 Technical Symposium on Optics, Electro-Optics, and Sensors*, p. 2, Orlando, Fla, USA, April 1990.

[4] X.-H. Xu, X.-D. Han, B. Wang, H.-K. Wang, and X.-Y. Zhuang, "Design of fast steering mirror with rigid support structure for airborne platform," *Guangxue Jingmi Gongcheng/Optics and Precision Engineering*, vol. 24, no. 1, pp. 126–133, 2016.

[5] H. Marth, M. A. Ealey, M. Donat, and C. F. Pohlhammer, "Latest experience in design of piezoelectric-driven fine-steering mirrors," in *Proceedings of the San Diego - DL tentative*, vol. 14, p. 248, San Diego, Calif, USA, 1992.

[6] A. Bullard and I. Shawki, "Responder fast steering mirror," in *SPIE Optical Engineering + Applications*, p. 6, 2013.

[7] C. Deng, T. Tang, Y. Mao, and G. Ren, "Enhanced disturbance observer based on acceleration measurement for fast steering mirror systems," *IEEE Photonics Journal*, vol. 9, no. 3, pp. 1–11, 2017.

[8] J. Tian, W. Yang, Z. Peng, T. Tang, and Z. Li, "Application of MEMS accelerometers and gyroscopes in fast steering mirror control systems," *Sensors*, vol. 16, no. 4, p. 440, 2016.

[9] Y. Hori, "A Review of torsional vibration control methods and a proposal of disturbance observer-based new techniques," *IFAC Proceedings Volumes*, vol. 29, no. 1, pp. 990–995, 1996.

[10] T. Egami and T. Tsuchiya, "Disturbance suppression control with preview action of linear DC brushless motor," *IEEE Transactions on Industrial Electronics*, vol. 42, no. 5, pp. 494–500, 1995.

[11] C.-S. Liu and H. Peng, "Disturbance observer based tracking control," *Journal of Dynamic Systems, Measurement, and Control*, vol. 122, no. 2, pp. 332–335, 2000.

[12] B. Yao, M. Al-Majed, and M. Tomizuka, "High-performance robust motion control of machine tools: An adaptive robust

control approach and comparative experiments," *IEEE/ASME Transactions on Mechatronics*, vol. 2, no. 2, pp. 63–76, 1997.

[13] Y. Bin, *Adaptive Robust Control of Nonlinear Systems with Application to Control of Mechanical Systems, Doctor of Philosophy dissertation, Mechanical Engineering [Phd. thesis]*, University of California at Berkeley, 1996.

[14] B. Yao and M. Tomizuka, "Adaptive Robust Control of Non linear Systems: Effective Use of Information," *IFAC Proceedings Volumes*, vol. 30, no. 11, pp. 873–878, 1997.

[15] J. E. Slotine and W. Li, "Adaptive manipulator control: a case study," *IEEE Transactions on Automatic Control*, vol. 33, no. 11, pp. 995–1003, 1988.

[16] B. Yao and M. Tomizuka, "Smooth robust adaptive sliding mode control of manipulators with guaranteed transient performance," *Journal of Dynamic Systems, Measurement, and Control*, vol. 118, no. 4, pp. 764–775, 1996.

[17] V. I. Utkin, "Variable structure systems with sliding modes," *IEEE Transactions on Automatic Control*, vol. 22, no. 2, pp. 212–222, 1977.

[18] K.-K. D. Young, "Controller design for a manipulator using theory of variable structure systems," *IEEE Transactions on Systems, Man, and Cybernetics*, vol. 8, no. 2, pp. 101–109, 1978.

[19] V. Utkin and L. Hoon, "Chattering problem in sliding mode control systems," in *Proceedings of the International Workshop on Variable Structure Systems, 2006. VSS'06*, pp. 346–350, 2006.

[20] K. D. Young, V. I. Utkin, and U. Ozguner, "A control engineer's guide to sliding mode control," in *Proceedings of the 1996 IEEE International Workshop on Variable Structure Systems, 1996. VSS '96*, vol. 27, pp. 1–14, 1996.